VIP NMR Spectroscopy Very Important Paper

International Edition: DOI: 10.1002/anie.201507831
German Edition: DOI: 10.1002/ange.201507831

2D NMR Trace Analysis by Continuous Hyperpolarization at High Magnetic Field

*Nan Eshuis, Ruud L. E. G. Aspers, Bram J. A. van Weerdenburg, Martin C. Feiters, Floris P. J. T. Rutjes, Sybren S. Wijmenga, and Marco Tessari**

Abstract: *Nuclear magnetic resonance is often the technique of choice in chemical analysis because of its sensitivity to molecular structure, quantitative character, and straightforward sample preparation. However, determination of trace analytes in complex mixtures is generally limited by low sensitivity and extensive signal overlap. Here, we present an approach for continuous hyperpolarization at high magnetic field that is based on signal amplification by reversible exchange (SABRE) and can be straightforwardly incorporated in multidimensional NMR experiments. This method was implemented in a 2D correlation experiment that allows detection and quantification of analytes at nanomolar concentration in complex solutions.*

Although NMR has gained a prominent role in chemical analysis over the last decades, investigation of dilute components still suffers from the relatively poor sensitivity of the technique. This limitation is further aggravated by the low dispersion of proton NMR resonances, which, in the case of complex mixtures, results in extensive signal overlap. As of today, NMR investigation and quantification of analytes below 20 μM remains a difficult task for challenging systems such as biofluids and natural extracts. Nuclear spin hyperpolarization methods in solution, such as dissolution dynamic nuclear polarization (dissolution DNP),[1] and signal amplification by reversible exchange (SABRE)[2] have been previously exploited in the context of mixture analysis to boost NMR sensitivity.[3] However, fast ^{1}H relaxation has so far limited the application of dissolution-DNP to heteronuclear NMR (mainly ^{13}C), which, for natural systems, requires relatively high analyte concentrations (typically millimolar). In contrast, SABRE allows NMR detection at sub-micromolar concentration,[4] albeit limited to species that can reversibly bind to an iridium-based metal complex in solution, as already shown for nucleobases,[5] amino acids,[6] drugs,[7] and tagged oligopeptides.[8] Furthermore, as SABRE relies on the reversible interactions of para-hydrogen (p-H_2) and substrate molecules at the metal complex, fast sample repolarization is possible by bubbling p-H_2 through solution.[5,9]

Here, we employ continuous hyperpolarization at high magnetic field for acquisition of 2D NMR spectra of complex mixtures in the nanomolar concentration regime. This experiment is fundamentally different from recently proposed high-field SABRE methods,[10] as it targets exclusively bound substrate molecules, and it does not require the matching of stringent conditions by selective radiofrequency irradiation.[10a–c] Therefore, it can provide the correlations of all SABRE complexes in solution at once, in a single spectrum. The combination of enhanced sensitivity from p-H_2-derived hyperpolarization and increased signal dispersion from multidimensional NMR spectroscopy, allows investigation of complex solutions far below conventional 2D NMR detection limits.

We have previously demonstrated that a large excess of metal ligand (referred to as "co-substrate") is necessary to preserve the efficiency of SABRE when the substrate under investigation is highly dilute.[4] The approach we here present depends on the structural asymmetry of co-substrate complexes (Figure 1).

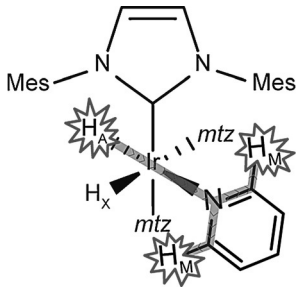

Figure 1. Schematic representation of the asymmetric [Ir(IMes)(H)$_2$-(mtz)$_2$(sub)]Cl complex for a pyridine-like substrate (sub) in the presence of a large excess of 1-methyl-1,2,3-triazole (mtz) as co-substrate. Only hydride H_A, trans with respect to the substrate, displays an appreciable scalar coupling interaction with substrate protons H_M, indicated by the arrows.

For such asymmetric complexes, the two hydride ligands resulting from p-H_2 binding (H_A and H_X in Figure 1) are not chemically equivalent, which determines fast singlet–triplet mixing at high magnetic field. Since p-H_2 binding and dissociation occur asynchronously for the metal complexes in the sample, oscillating components of the hydrides' singlets (i.e. zero-quantum coherence) are rapidly dephased.[11] The surviving singlet term, longitudinal spin order, can be converted to enhanced hydride NMR signals, as previously proposed by Woods et al.[12] Alternatively, enhanced hydride

[*] N. Eshuis, Ing. R. L. E. G. Aspers, B. J. A. van Weerdenburg, Dr. M. C. Feiters, Prof. Dr. F. P. J. T. Rutjes, Prof. Dr. S. S. Wijmenga, Dr. M. Tessari
Radboud University, Institute for Molecules and Materials
Heyendaalseweg 135, Nijmegen, 6525 AJ (Netherlands)
E-mail: m.tessari@science.ru.nl

Supporting information for this article is available on the WWW under http://dx.doi.org/10.1002/anie.201507831.

magnetization has been exploited to characterize metal dihydride complexes by 2D heteronuclear NMR spectroscopy.[13] Here, the spin-order of the hydrides is used to enhance the NMR signals of substrate protons in the metal complex by long-range scalar couplings. Being performed at high field, no sample transfer is required, which allows for rapid acquisition of multiple scans of continuously hyperpolarized spectra.

This is illustrated by the 2D NMR spectrum in Figure 2 A recorded in 23 minutes for a mixture of thirteen SABRE

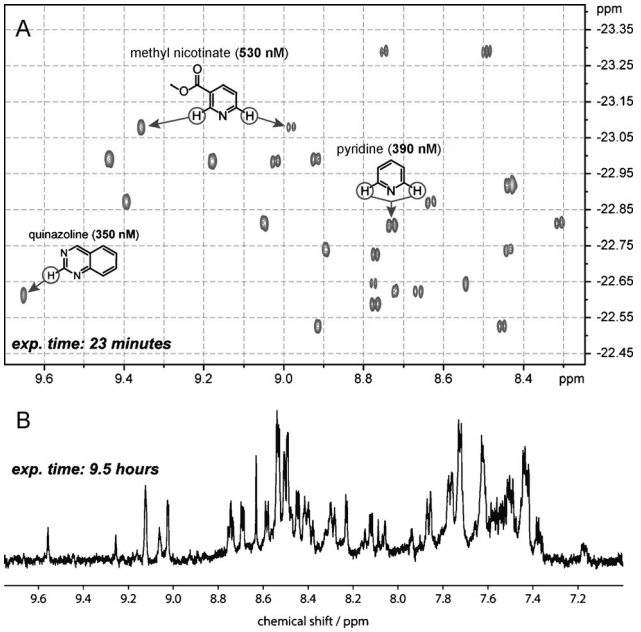

Figure 2. A) 2D ^{1}H-^{1}H correlation spectrum between enhanced hydrides and aromatic protons of a mixture of thirteen SABRE substrates with concentrations between 250 nM and 2 μM (see the Supporting Information). The spectrum was recorded in 23 minutes at 25 °C in the presence of 2 mM metal complex, 30 mM mtz, 5 bar 51% enriched p-H_2. B) 1D spectrum of the same substrates mixture, in the absence of metal complex, mtz, and p-H_2. This spectrum was acquired with 32 768 scans in 9.5 h using a 30-degree pulse and a recovery delay of 1 s. Both spectra were acquired at 500 MHz, ^{1}H resonance frequency.

substrates at concentrations between 250 nM and 2 μM. All overlapping substrate resonances are nicely resolved in the 2D correlation spectrum thanks to the high dispersion of the hydride signals. Note that 2D SABRE experiments reported so far operate at concentrations that are approximately two orders of magnitude higher than in the present case.[2e,14]

The conventional ^{1}H spectrum in Figure 2 B illustrates the sensitivity gain offered by our high field hyperpolarization approach. This spectrum was acquired on the same substrate mixture employed for the 2D experiment. However, for the fairness of the comparison, it was recorded in the absence of catalyst and without de-oxygenating the sample to shorten longitudinal relaxation times. Nevertheless, it took 9.5 h to achieve a signal-to-noise ratio sufficient for spectral analysis. Still, extensive signal crowding prevents a reliable identification and quantification for most resonances. All signals observed in this 1D reference spectrum derive from protons

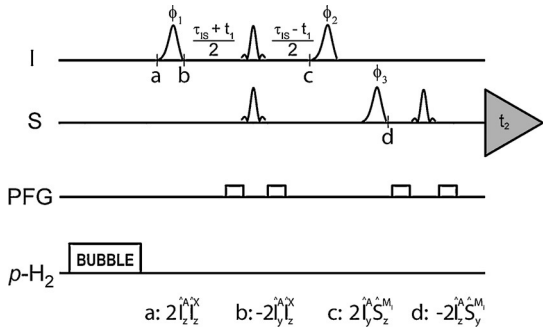

Figure 3. Pulse scheme used for the hyperpolarization transfer from the hydrides (I) to the protons of the substrate (S). Shaped pulses are eburp-1 for excitation and reburp for refocusing/inversion (see the Supporting Information for pulse parameters). The delay τ_{IS} is taken as an odd multiple of $1/(2*J_{AX})$, where J_{AX} ($\approx$8 Hz) is the (average) hydride–hydride coupling constant. The duration here employed (185 ms) allows for an efficient coherence transfer to the substrate protons in ortho. Relevant terms of the density operator at time points "a", "b", "c", and "d" are indicated. Bubbling p-H_2 through the sample (typically 1 s) occurs under spectrometer control, at the beginning of each transient. Phase cycling is implemented as follows: $\phi_1 = x,-x$; $\phi_2 = x,x,-x,-x$; $\phi_3 = x,x,x,x,-x,-x,-x,-x$; $\phi_{receiver} = x,-x,-x,x,-x,x,x,-x$.

of the substrates free in solution. Therefore, their resonance frequencies differ from those observed in the 2D correlation spectrum.

The pulse scheme sketched in Figure 3 was used to acquire the 2D NMR correlation spectrum between hydrides and substrate protons. Bubbling p-H_2 at high field results in hydride longitudinal spin order (time point "a" in Figure 3) that is converted into antiphase coherence by the first selective 90-degree pulse (point "b"). Offset and bandwidth of this pulse are optimized to selectively excite only hydride H_A that is *trans* with respect to the substrate (Figure 1).[15] During the Constant-Time evolution period τ_{IS} this antiphase term is refocused, while antiphase with respect to the substrate protons H_{M_i} is created by long-range couplings (point "c"). A pair of 90-degree selective pulses transfers the coherence to the substrate protons for detection (point "d"). Because of the sine-modulation of the acquired signal, these correlation spectra should be processed in magnitude-mode for a quantitative analysis. In summary, the coherence flow from hydride H_A (I^A) to substrate proton H_{M_i} (S^{M_i}) can be described by means of product operator formalism as Equation (1),

$$
\begin{aligned}
&2\hat{I}_z^{\mathrm{A}}\hat{I}_z^{\mathrm{X}} \xrightarrow{\left(\frac{\pi}{2}\right)_x^{I^A}} -2\hat{I}_y^{\mathrm{A}}\hat{I}_z^{\mathrm{X}} \\
&\xrightarrow{\tau_{IS}} 2\hat{I}_y^{\mathrm{A}}\hat{S}_z^{\mathrm{M}_i}\exp\left(-\left(\frac{1}{T_2^{\mathrm{hydr}}}+\frac{1}{\tau_{\mathrm{complex}}}\right)\tau_{IS}\right)\sin(\pi J_{\mathrm{AX}}\tau_{IS})\sin(\pi J_{\mathrm{AM}_i}\tau_{IS}) \\
&\cos(\omega_{\mathrm{H_A}}t_1)\prod_{j\neq i}\cos(\pi J_{\mathrm{AM}_j}\tau_{IS}) \xrightarrow{\left(\frac{\pi}{2}\right)_x^{I^A},\left(\frac{\pi}{2}\right)_x^{S}} -2\hat{I}_z^{A}\hat{S}_y^{M_i}\exp\left(-\left(\frac{1}{T_2^{\mathrm{hydr}}}+\frac{1}{\tau_{\mathrm{complex}}}\right)\tau_{IS}\right) \\
&\sin(\pi J_{\mathrm{AX}}\tau_{IS})\sin(\pi J_{\mathrm{AM}_i}\tau_{IS})\cos(\omega_{\mathrm{H_A}}t_1)\prod_{j\neq i}\cos(\pi J_{\mathrm{AM}_j}\tau_{IS})
\end{aligned}
\tag{1}
$$

where J_{AX} is the hydride–hydride coupling, while J_{AM_i} and J_{AM_j} indicate the long-range active and passive couplings between

hydride H_A and substrate proton spins H_{M_i} and H_{M_j}, respectively. The symbols T_2^{hydr} and $\tau_{complex}$ refer to hydride transverse relaxation time and complex lifetime, respectively.

We have previously shown that calibration techniques can be used in combination with SABRE hyperpolarization for a quantitative determination of dilute analytes in solution by 1D NMR spectroscopy.[3c] Also for the proposed high-field approach, the 2D signals are linearly dependent on substrate concentration, provided a large excess of co-substrate is present. However, the antiphase character of the acquired signals requires particular consideration, since variations in peak linewidths because of instrumental instabilities might affect resonances integrals thus potentially compromising a quantitative NMR analysis.[16] Nevertheless, from the comparison of a series of repeated measurements we found that the variations in signals integrals are consistent with the root-mean-square-deviation (RMSD) noise of the spectra, suggesting negligible effects of magnetic field inhomogeneity (see the Supporting Information).

The robustness of our approach is likewise reflected in the accuracy of the concentrations obtained by standard addition method for four substrates in the dilute mixture previously employed. The linear plots of the 2D signal integrals versus added substrate concentration are shown in Figure 4. Substrate concentrations, estimated from the average value of the abscissa intercepts, are in good agreement with the nominal values. As shown in Equation (1), the coherence transfer efficiency is determined by the interplay of scalar couplings, relaxation and dissociation rates. In addition, the signal integral is influenced by the substrate binding affinity: for the mixture under investigation, the molar fraction of bound substrates varied between 0.25 and 0.65. The combined effect of these variables is reflected in the different slopes observed in the standard addition experiments.

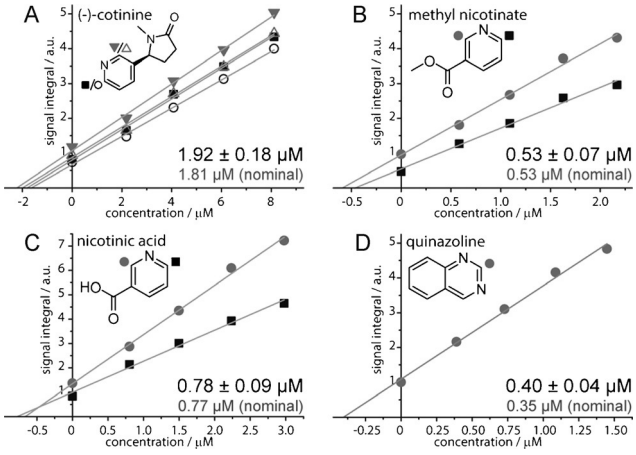

Figure 4. Standard addition curves for (−)-cotinine (**A**), methyl nicotinate (**B**), nicotinic acid (**C**), and quinazoline (**D**). Experimental uncertainties were derived by error propagation. The symbols used in the graphs refer to different protons, as indicated on the molecular structures. Note that each (−)-cotinine proton results in two resonances when bound to iridium because of formation of diastereomeric complexes (see the Supporting Information).

In conclusion, we have presented a method to detect and quantitate SABRE substrates at sub-micromolar concentrations in solution, by 2D NMR correlations with hydride ligands. Because of their superior dispersion, hydrides allow to efficiently spread overlapping substrate resonances in two dimensions, which is of crucial importance for quantitative analysis in complex mixtures. The continuous signal enhancement provided by p-H_2 at high magnetic field depends on the asymmetric structure of the SABRE hyperpolarization transfer complex, and allows rapid, in situ acquisition of 2D spectra at nanomolar concentrations. Note that an additional threefold sensitivity increase could be achieved by using fully enriched p-H_2, which should further reduce the experimental time.[17] However, single-scan 2D acquisition will be limited to samples at higher concentrations, because of the high sensitivity requirements of the ultrafast method.[2e,3a,14,16] The previously demonstrated linearity of SABRE signals with concentration[3c] applies also to the present 2D approach, and provides an accurate concentration determination in the nanomolar regime.

We believe that this combination of p-H_2-based signal enhancement and 2D NMR resonance dispersion offers a powerful tool for trace analysis of complex mixtures.

Experimental Section

Asymmetric metal complexes $[Ir(IMes)(H)_2(mtz)_2(sub)]Cl$ (IMes = 1,3-bis(2,4,6-trimethylphenyl)imidazole-2-ylidene, mtz = 1-methyl-1,2,3-triazole, sub = substrate) were formed by dissolving molecular hydrogen in a $[D_4]$MeOH solution containing 1.3 mg mL^{-1} complex precursor Ir(COD)(IMes)Cl (COD = cyclooctadiene), in the presence of a 15-fold excess of co-substrate mtz, and thirteen substrates at low- to submicromolar concentrations. p-H_2 was bubbled through the solution in situ using an in-house designed sample cell. More details on chemicals, sample preparation, bubbling setup, and NMR experiments can be found in the Supporting Information.

Acknowledgements

We thank Dr. Hans Heus for his helpful comments and the European Union and the provinces of Gelderland and Overijssel for support in the EFRO Ultrasense NMR project.

Keywords: hyperpolarization · multidimensional NMR spectroscopy · para-hydrogen · signal amplification · trace analysis

How to cite: *Angew. Chem. Int. Ed.* **2015**, *54*, 14527–14530
Angew. Chem. **2015**, *127*, 14735–14738

[1] a) J. H. Ardenkjær-Larsen, B. Fridlund, A. Gram, G. Hansson, L. Hansson, M. H. Lerche, R. Servin, M. Thaning, K. Golman, *Proc. Natl. Acad. Sci. USA* **2003**, *100*, 10158–10163; b) J. Wolber, F. Ellner, B. Fridlund, A. Gram, H. Jóhannesson, G. Hansson, L. H. Hansson, M. H. Lerche, S. Månsson, R. Servin, M. Thaning, K. Golman, J. H. Ardenkjær-Larsen, *Nucl. Instrum. Methods Phys. Res. Sect. A* **2004**, *526*, 173–181; c) L. Frydman, D. Blazina, *Nat. Phys.* **2007**, *3*, 415–419.

[2] a) R. W. Adams, J. A. Aguilar, K. D. Atkinson, M. J. Cowley, P. I. P. Elliott, S. B. Duckett, G. G. R. Green, I. G. Khazal, J. Lopez-Serrano, D. C. Williamson, *Science* **2009**, *323*, 1708–1711;

b) R. W. Adams, S. B. Duckett, R. A. Green, D. C. Williamson, G. G. R. Green, *J. Chem. Phys.* **2009**, *131*, 194505; c) M. J. Cowley, R. W. Adams, K. D. Atkinson, M. C. R. Cockett, S. B. Duckett, G. G. Green, J. A. B. Lohman, R. Kerssebaum, D. Kilgour, R. E. Mewis, *J. Am. Chem. Soc.* **2011**, *133*, 6134 – 6137; d) E. B. Dücker, L. T. Kuhn, K. Münnemann, C. Griesinger, *J. Magn. Reson.* **2012**, *214*, 159 – 165; e) L. S. Lloyd, R. W. Adams, M. Bernstein, S. Coombes, S. B. Duckett, G. G. Green, R. J. Lewis, R. E. Mewis, C. J. Sleigh, *J. Am. Chem. Soc.* **2012**, *134*, 12904 – 12907; f) B. J. A. van Weerdenburg, S. Glöggler, N. Eshuis, A. H. J. Engwerda, J. M. M. Smits, R. de Gelder, S. Appelt, S. S. Wymenga, M. Tessari, M. C. Feiters, B. Blumich, F. P. J. T. Rutjes, *Chem. Commun.* **2013**, *49*, 7388 – 7390; g) T. Theis, M. L. Truong, A. M. Coffey, R. V. Shchepin, K. W. Waddell, F. Shi, B. M. Goodson, W. S. Warren, E. Y. Chekmenev, *J. Am. Chem. Soc.* **2015**, *137*, 1404 – 1407; h) R. V. Shchepin, M. L. Truong, T. Theis, A. M. Coffey, F. Shi, K. W. Waddell, W. S. Warren, B. M. Goodson, E. Y. Chekmenev, *J. Phys. Chem. Lett.* **2015**, *6*, 1961 – 1967; i) K. X. Moreno, K. Nasr, M. Milne, A. D. Sherry, W. J. Goux, *J. Magn. Reson.* **2015**, *257*, 15 – 23.

[3] a) P. Giraudeau, Y. Shrot, L. Frydman, *J. Am. Chem. Soc.* **2009**, *131*, 13902 – 13903; b) J.-N. Dumez, J. Milani, B. Vuichoud, A. Bornet, J. Lalande-Martin, I. Tea, M. Yon, M. Maucourt, C. Deborde, A. Moing, L. Frydman, G. Bodenhausen, S. Jannin, P. Giraudeau, *Analyst* **2015**, *140*, 5860 – 5863; c) N. Eshuis, B. J. A. van Weerdenburg, M. C. Feiters, F. P. J. T. Rutjes, S. S. Wijmenga, M. Tessari, *Angew. Chem. Int. Ed.* **2015**, *54*, 1481 – 1484; *Angew. Chem.* **2015**, *127*, 1501 – 1504.

[4] N. Eshuis, N. Hermkens, B. J. A. van Weerdenburg, M. C. Feiters, F. P. J. T. Rutjes, S. S. Wijmenga, M. Tessari, *J. Am. Chem. Soc.* **2014**, *136*, 2695 – 2698.

[5] J.-B. Hövener, N. Schwaderlapp, T. Lickert, S. B. Duckett, R. E. Mewis, L. A. R. Highton, S. M. Kenny, G. G. R. Green, D. Leibfritz, J. G. Korvink, J. Hennig, D. von Elverfeldt, *Nat. Commun.* **2013**, *4*, 2946 – 2950.

[6] S. Glöggler, R. Muller, J. Colell, M. Emondts, M. Dabrowski, B. Blümich, S. Appelt, *Phys. Chem. Chem. Phys.* **2011**, *13*, 13759 – 13764.

[7] a) H. Zeng, J. Xu, J. Gillen, M. T. McMahon, D. Artemov, J.-M. Tyburn, J. A. B. Lohman, R. E. Mewis, K. D. Atkinson, G. G. R. Green, S. B. Duckett, P. C. M. van Zijl, *J. Magn. Reson.* **2013**, *237*, 73 – 78; b) S. Glöggler, M. Emondts, J. Colell, R. Müller, B. Blümich, S. Appelt, *Analyst* **2011**, *136*, 1566 – 1568.

[8] T. Ratajczyk, T. Gutmann, P. Bernatowicz, G. Buntkowsky, J. Frydel, B. Fedorczyk, *Chem. Eur. J.* **2015**, *21*, 12616 – 12619.

[9] J.-B. Hövener, S. Knecht, N. Schwaderlapp, J. Hennig, D. von Elverfeldt, *ChemPhysChem* **2014**, *15*, 2451 – 2457.

[10] a) A. N. Pravdivtsev, A. V. Yurkovskaya, H. M. Vieth, K. L. Ivanov, *Phys. Chem. Chem. Phys.* **2014**, *16*, 24672 – 24675; b) T. Theis, M. Truong, A. M. Coffey, E. Y. Chekmenev, W. S. Warren, *J. Magn. Reson.* **2014**, *248*, 23 – 26; c) A. N. Pravdivtsev, A. V. Yurkovskaya, H. M. Vieth, K. L. Ivanov, *J. Phys. Chem. B* **2015**, DOI: 10.1021/acs.jpcb.5b03032; d) D. A. Barskiy, K. V. Kovtunov, I. V. Koptyug, P. He, K. A. Groome, Q. A. Best, F. Shi, B. M. Goodson, R. V. Shchepin, A. M. Coffey, K. W. Waddell, E. Y. Chekmenev, *J. Am. Chem. Soc.* **2014**, *136*, 3322 – 3325.

[11] a) C. R. Bowers, D. P. Weitekamp, *Phys. Rev. Lett.* **1986**, *57*, 2645 – 2648; b) O. Torres, B. Procacci, M. E. Halse, R. W. Adams, D. Blazina, S. B. Duckett, B. Eguillor, R. A. Green, R. N. Perutz, D. C. Williamson, *J. Am. Chem. Soc.* **2014**, *136*, 10124 – 10131.

[12] N. J. Wood, J. A. Brannigan, S. B. Duckett, S. L. Heath, J. Wagstafft, *J. Am. Chem. Soc.* **2007**, *129*, 11012 – 11013.

[13] a) S. B. Duckett, G. K. Barlow, M. G. Partridge, B. A. Messerle, *J. Chem. Soc. Dalton Trans.* **1995**, 3427 – 3429; b) C. J. Sleigh, S. B. Duckett, B. A. Messerle, *Chem. Commun.* **1996**, 2395 – 2396; c) B. A. Messerle, C. J. Sleigh, M. G. Partridge, S. B. Duckett, *J. Chem. Soc. Dalton Trans.* **1999**, 1429 – 1435.

[14] V. Daniele, F.-X. Legrand, P. Berthault, J.-N. Dumez, G. Huber, *ChemPhysChem* **2015**, DOI: 10.1002/cphc.201500535.

[15] a) H. Sengstschmid, R. Freeman, J. Barkemeyer, J. Bargon, *J. Magn. Reson. Ser. A* **1996**, *120*, 249 – 257; b) J. Barkemeyer, J. Bargon, H. Sengstschmid, R. Freeman, *J. Magn. Reson. Ser. A* **1996**, *120*, 129 – 132; c) J. Natterer, J. Bargon, *Prog. Nucl. Magn. Reson. Spectrosc.* **1997**, *31*, 293 – 315.

[16] P. Giraudeau, S. Massou, Y. Robin, E. Cahoreau, J.-C. Portais, S. Akoka, *Anal. Chem.* **2011**, *83*, 3112 – 3119.

[17] B. Feng, A. M. Coffey, R. D. Colon, E. Y. Chekmenev, K. W. Waddell, *J. Magn. Reson.* **2012**, *214*, 258 – 262.

Received: August 12, 2015
Revised: September 11, 2015
Published online: October 6, 2015

